10.17951/aa.2019.74.2.1-24

ANNALES
UNIVERSITATIS MARIAE CURIE-SKŁODOWSKA
LUBLIN – POLONIA

VOL. LXXIV, 2 SECTIO AA 2019

Visual presentation of the correlation between solid surface free energy and its wettability by flotation tests using the Hallimond tube

Lucyna Hołysz* and Emil Chibowski

Institute of Chemical Sciences, Faculty of Chemistry,
Department of Interfacial Phenomena, Maria Curie Skłodowska University,
Maria Curie-Skłodowska Sq. 3, 20-031 Lublin, Poland
**email: lucyna.holysz@umcs.pl*

This paper presents earlier published results, as well some new ones, of the flotation tests carried out with the help of a Hallimond tube for several different apolar and polar solids (minerals and rocks). This is to depict the relationship between solid surface free energy and its flotability. Although the thermodynamic condition for the efficient flotation of a solid is well known, this paper prompts the not-acquainted readers to get familiar with the fundamental thermodynamic relationships involved in the wetting processes and to learn about usefulness of the simple flotation experiments for this purpose. This relationship between the flotation recovery of a solid and the work of water spreading on the solid surface is clearly illustrated. The work of spreading is the difference between the work of adhesion and the work of water cohesion. This work has to be negative to carry out an efficient flotation of a solid sample. Thus, the purpose of this paper is to show that the simple Hallimond tube is a very useful laboratory tool for studying mineral and rock surface hydrophobic/hydrophilic character under the kinetic conditions.

1. INTRODUCTION

Hallimond tube is the simplest tool to study solid grains flotation in the laboratory conditions [1–14]. The basic act of flotation is solid particle attachment to a gas bubble. Drelich [15] formulated three general criteria needed for this process to form a stable particle-bubble aggregate in the kinetic condition. Namely: i) the mineral surface must acquire stronger affinity to the gas phase than to the aqueous phase, and the area of solid/air contact must be of sufficient dimension, ii) a minimal time is needed for the mineral particle and gas bubble to be in the interaction force field, iii) the hydrodynamic condition requires the particle/bubble aggregate must be sufficiently strong to be stable in the flow in the flotation cell. In case of a hydrophilic surface these conditions can be achieved using a suitable surfactant (collector) which adsorbing on the useful solid (mineral) surface converts it into a hydrophobic one [2, 4, 8, 13, 14, 16–28].

Therefore, the volume of gas and time needed to carry up given amount the particles to the surface depend on the solid surface free energy which determines the wetting of its surface by water. The thermodynamic condition for an efficient flotation is well known [29]. In short it occurs if the work of water adhesion is less than the work of its cohesion, i.e. the work of water spreading has to be negative [6, 30]. The work of spreading is the difference between the work of adhesion and the work of water cohesion which at 20°C amounts to 145.6 mJ/m^2. Besides a great applicability of the flotation method for minerals and/or rocks recovery, it can be also applied as a good tool for characterization of materials [31–33], or more generally, to investigate hydrophobicity under the kinetic conditions, especially wetting phenomena in the presence and/or absence of a surfactant [6, 30, 32, 34–38]. Drzymała et al. [35–38] applied the single-bubble Hallimond tube for determination of the gas bubble/water/solid particle contact angle which they called as ‘flotometric method’. According to them, the flotometry allows determination of the detachment (advancing) contact angle which can be recalculated into ‘the relaxed contact angle’. They consider this contact angle to be close to the Young equilibrium contact angle.

The goal of this paper is to prompt it students and/or readers who wish to get familiar with the fundamental thermodynamic relationships involved in the wetting processes to learn about

usefulness of simple flotation experiments for this purpose. However, by no means the paper deals with many above mentioned problems of a real flotation process. In this paper there are recalled the results published earlier in the Annales UMCS and elsewhere [2, 4, 6, 39–46]. Also some new results are included. Thus, these authors wished to depict again the usefulness of such simple experiments for visual testing of thermodynamic relationship between the surface free energy and the surface wetting via the flotation tests.

It should be mentioned that in laboratory investigations to study flotation and accompanying processes the original Hallimond tube [1, 2, 11, 31–33, 48] and its various modifications [3; 8, 16, 22, 49–51] was often used.

2. THERMODYNAMIC CONDITIONS FOR FLOTATION

Although it is well described in the literature [52] the thermodynamics of single flotation act which relies in the replacement of the particle/liquid interface by the particle/gas interface, which results in the solid (mineral, rock) grain attachment to the gas bubble, nevertheless for the sake of clarity it is worthy to recall these fundamental relationships (Fig. 1).

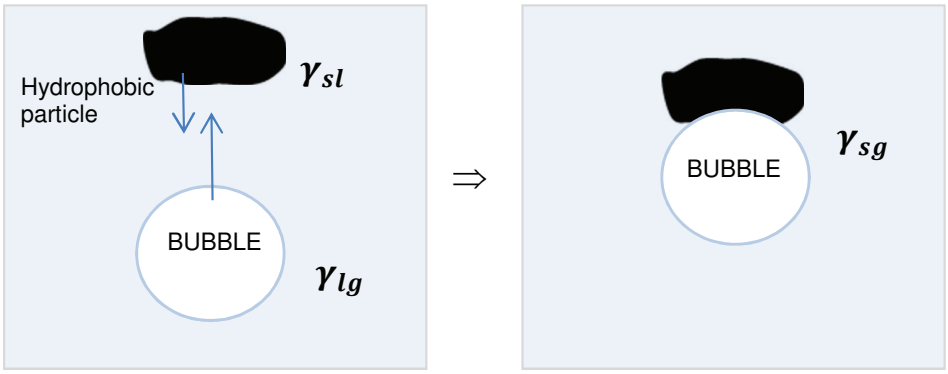

Fig. 1. Schematic presentation of a gas bubble attachment in water to hydrophobic particle for negative the free energy of interaction.

This process can be depicted following [6]:

$$\text{particle/water} \Leftrightarrow \text{water/gas} \Rightarrow \text{particle/gas}$$
$$\gamma_{SL} + \gamma_{LG} \rightarrow \gamma_{SG}$$

and it is described by the Dupre's equation:

$$\Delta G = \gamma_{SG} - (\gamma_{LG} + \gamma_{SL}) \quad (1)$$

where ΔG is the Gibbs free energy accompanying the attachment process, γ_{SG} is the solid surface free energy, γ_{LG} is the liquid surface free energy (surface tension), and γ_{SL} is the solid/liquid interfacial free energy. Obviously for the process to occur spontaneously the free energy change ΔG has to be negative [29, 52]. The interfacial solid/liquid free energy is expressed by Eq. (2) [53]:

$$\gamma_{SL} = \gamma_S + \gamma_L - W_A \quad (2)$$

where W_A is the work of adhesion of a liquid to the solid surface. Note, in Eq. (2) for clarity the subscript G (gas) at the symbol γ of solid and liquid surface free energy has been neglected. The same will be applied to the remaining part of the equations. Then by inserting Eq. (2) into Eq. (1) it results that ΔG equals to the work of water spreading W_S:

$$\Delta G = \gamma_S - \gamma_L - \gamma_{SL} = \gamma_S - \gamma_L - \gamma_S - \gamma_L + W_A \quad (3)$$

$$\Delta G = W_A - W_C = W_S \quad (4)$$

where $W_C = 2\gamma_L$ is the work of cohesion. Equation 4 points out that the adhesion of a gas bubble to a solid grain is possible if the work of liquid (water) cohesion W_C (145.6 mJ/m^2 at 20°C) is greater than the work of liquid adhesion W_A to the solid surface. This indicates that the work of water spreading on the mineral surface must be negative. Therefore, to learn whether the solid particle/gas bubble stable adhesion will occur, the work of water adhesion has to be known in order to calculate the free energy change ΔG. In the solid/liquid systems where the liquid forms a droplet, the work of adhesion W_A can be determined easily via measurement of the liquid (water) contact angle θ on the mineral smooth surface. Then from the Young-Dupre's equation [54, 55] it can be expressed as:

$$\gamma_S = \gamma_L cos\theta + \gamma_{SL} = \gamma_L cos\theta + \gamma_S + \gamma_L - W_A \quad (5)$$

$$W_A = \gamma_L(1 + cos\theta) \quad (6)$$

and because the work of spreading $W_S = W_A - W_C = W_A - 2\gamma_L$, hence:

$$W_S = \gamma_L(cos\theta - 1) = \Delta G \quad (7)$$

The work of adhesion and work of spreading result from the interfacial interactions which can be described in different ways, depending on the theoretical approach.

For example, based on the Owens and Wendt's (O-W) approach [56] it is assumed that the surface free energy (γ_i) is a sum of two components. One is apolar γ_i^d, resulting from the dispersive interactions only and the another is polar γ_i^p, related to all kinds of the interactions other than the dispersive ones. Consequently, the thermodynamic work of adhesion W_A at the solid/liquid interface is described following:

$$W_A = \gamma_L(1 + cos\theta) = 2\left(\gamma_L^d \gamma_S^d\right)^{1/2} + 2\left(\gamma_L^p \gamma_S^p\right)^{1/2} \quad (8)$$

where the subscripts *S* and *L* mean the solid and liquid, respectively.

Next, according to the approach proposed by van Oss et al. [57] (Lifshitz-van der Waals and acid-base approach – LWAB), in which γ_i is expressed as a sum of apolar interactions γ_i^{LW} (called the Lifshitz-van der Waals) and polar interactions γ_i^{AB} (the Lewis acid-base), the work of adhesion W_A of a liquid to a solid surface is expressed:

$$W_A = \gamma_L(1 + cos\theta_a) = 2(\gamma_S^{LW}\gamma_L^{LW})^{1/2} + 2(\gamma_S^+\gamma_L^-)^{1/2} + 2(\gamma_S^-\gamma_L^+)^{1/2} \quad (9)$$

where γ_S^+ and γ_L^+ are the electron-acceptor and γ_S^- and γ_L^- are the electron-donor parameters of the acid-base component of surface free energy of solid and liquid.

As follows from Eqs. (8) and (9), having determined the work of adhesion from contact angles of probe liquids on the solid (mineral, rock) surface, its surface free energy components can be calculated [42, 46, 58–60]. However, in the case where a smooth solid (mineral or rock) surface cannot be obtained, e.g. because the mineral is dispersed in a rock, the compressed pellets of its powder can be applied [43, 61]. Also a method based on the zeta potential measurements for a series of solid samples [2, 4, 41–43, 46], and the thin layer wicking (TLW) [45, 62] or thin column wicking (TLC) [6] techniques were used. Lately Rudolph and Hartman [30] have applied inverse gas chromatography for determination of powdered minerals (quartz, fluoroapatite and magnetite) surface free energy and correlated with their minerals flotability.

Thus, to sum up, if the work of water adhesion to the solid surface is determined, from contact angle measurement or the

surface free energy components, then the Gibbs' free energy ΔG accompanying the flotation process can be calculated too. In this paper the hydrophilic/hydrophobic characteristics of surface of different solids (resulting from the surface coverage with a collector) published earlier will be reported. Thus, the relationship between the solid surface free energy components, changes in the free energy ΔG, and flotability of the following minerals and rocks will be presented: sulfur/*n*-alkane [39, 40], coal/*n*-alkane [41, 46], quartz/DDACl [2], marble/TDACl, barite/TDACl [43, 44] and barite/SDS [4, 44].

3. HYDROPHOBIC SOLIDS: SULFUR AND COAL

Although some minerals and rocks are to some degree naturally hydrophobic, however, in the processes of their enrichment (flotation, agglomeration) a mixture of water-insoluble hydrocarbons is used as the collectors to increase the grains affinity to the air bubbles, e.g. in the case of coal which is organic rock [63, 64].

In practical systems even in the case of hydrophobic solid particle the presence of water film should be taken into account. The film creates an energy barrier between the solid particle and the gas bubble which has to be disrupt during the particle/gas aggregate formation. For this purpose water vapour adsorption on sulfur surface covered by *n*-alkanes (from *n*-hexane to *n*-hexadecane) and the sulfur flotation in a single-bubble Hallimond tube were investigated [39] (Fig. 1A and 1B).

The flotation activity of sulfur was expressed by volume of nitrogen needed for complete flotation of the sample. Fig. 1A shows that the amount of adsorbed water on the sulfur/*n*-alkanes films surface significantly decreases in comparison to the bare surface (the dotted line). There can be also seen differences in the adsorption of water vapour on the sulfur surface with the films of *n*-alkanes having even and odd numbers of carbon atoms in the chain. Similar oscillatory changes are observed in the flotation activity (Fig. 1B).

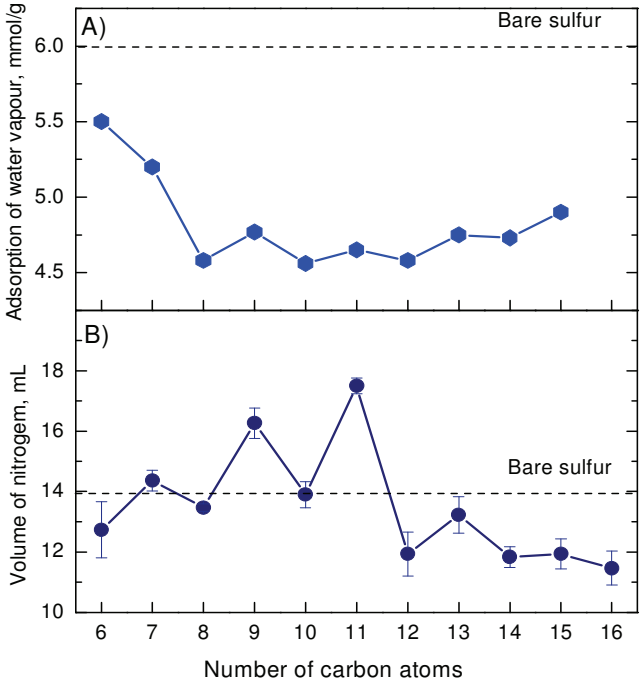

Fig. 1. A) Adsorption of water vapor on sulfur surface prewetted with *n*-alkanes against their chain length; B) Changes in nitrogen volume consumed for complete flotation of sulfur samples prewetted *n*-alkane (1 mm^3/1.5 g) Reproduced from Ref. [39].

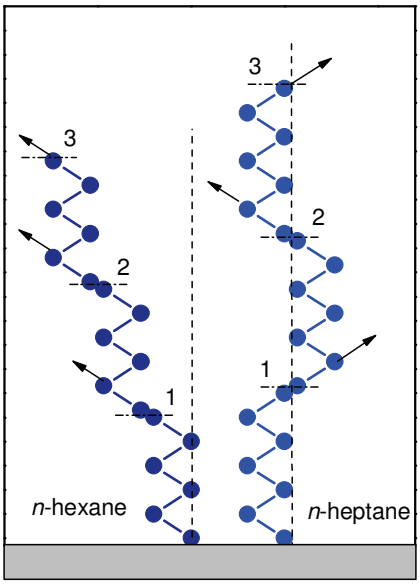

Fig. 2. Schematic presentation of differences in the structure of solid odd and even *n*-alkanes (*n*-hexane and *n*-heptane). Statistical monomolecular layers of *n*-alkanes are marked too. Reproduced from Ref. [40].

The changes correspond with those of their melting temperatures and results in differences in their structure in the solid state (Fig. 2) and they were found by X-ray spectroscopy [40]. The relationship in Fig. 1 shows that even for the hydrophobic surface, such as sulfur, the structure of water layer between the gas bubble and the sulfur/*n*-alkanes film surface under the kinetic conditions plays a significant role and determines sulphur flotation activity.

Similar correlations of flotation activity and water film thickness were also observed for sulfur covered with different amounts of *n*-heptane (Fig. 3). Fig. 3A shows the changes of nitrogen volume consumed for complete flotation of sulfur as a function of its surface coverage with *n*-heptane. The calculated monomolecular layers of the film are denoted in the figure (vertical orientation of *n*-heptane molecules (18 Å) was assumed). Moreover, the adsorbed amount of water vapour also correlates with the flotability changes (Fig. 3B) [39].

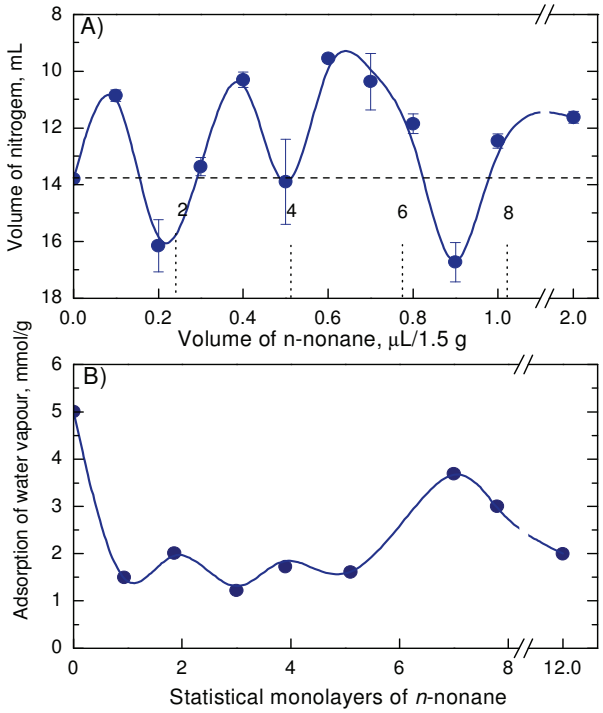

Fig. 3. A) Nitrogen volume consumed for complete flotation of sulfur samples as a function of the sulfur coverage with *n*-heptane; vertical dashed lines show the number of calculated monolayers of *n*-heptane; B) Changes in water vapor adsorption on sulfur surface at 20°C as a function of the sulfur coverage with *n*-heptane (statistical monolayers). Reproduced from Ref. [39].

Although, the coal surface (here according to PN-82-G-97002 a gas coal 33 from Nowy Wirek colliery, Poland was used) is less hydrophobic than that of sulfur, similar relationships between its flotability and the *n*-alkane surface coverage were obtained (Figs. 4 and 5) [41]. In Fig. 4 the flotation recovery of coal 33 precovered with 4 statistical (calculated) monolayers of given *n*-alkane against the number carbon atoms in the chain is plotted. There were step changes in the floatability of coal, which is characteristic of hydrophobic solids [39]. Moreover, similar changes of the contact angle on a graphite plate wetted with *n*-alkanes were found by Jańczuk [65].

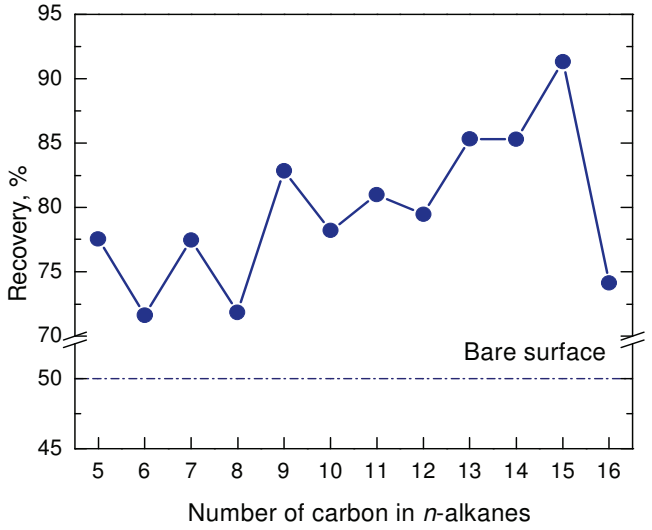

Fig. 4. Changes of recovery of coal 33 against carbon atom number in the *n*-alkane chain – the surface precovered with 4 statistical monolayers of these *n*-alkanes. (1.5 g samples floated with 100 mL of nitrogen). Reproduced from Ref. [41].

Then in Fig. 5 the coal recovery changes vs. *n*-nonane film thickness are presented, where recovery increases sharply from 50% to 82% at the surface coverage less than 1 statistical monolayer and further increases up to 85% at 5 monolayers to decrease sharply at the larger the surface coverage. This is due to the *n*-nonane film detachment from the grain surface by the gas bubble without its transport to the surface. The results in Figs. 4 and 5 show clearly that the surface hydrophobicity is determined by the kind of *n*-alkane and its film thickness. The surface free energy components were determined for the bare coal surface and then the work of spreading $W_S = W_A - W_C$ was calculated. A negative value of the spreading

work informs that the thermodynamic condition for the mineral flotation is fulfilled [41].

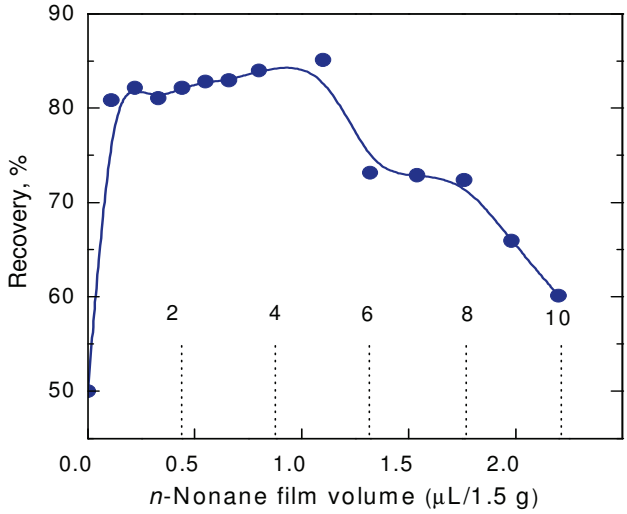

Fig. 5. Floatation recovery changes of coal 33 wetted with *n*-nonane; vertical dashed lines show the number of statistical monolayers of *n*-nonane (1.5 g samples floated with 100 mL of nitrogen). Reproduced from Ref. [41].

Analogous study was conducted for the other lower rank coals: flame coal 31 (31.1; 31.2) and gas flame coal 32 (32.1; 32.2) [46]. The surface free energy properties of these coals are summarized in Table 1.

Table 1. Surface free energy components of various type of coals calculated based on O-W and LWAB approaches, work of water spreading (W_S) and flotation recovery [46].

Type of coal	$\gamma_S^d=\gamma_S^{LW}$	γ_S^p	W_S	γ_S^-	γ_S^+	γ_S^{AB}	W_S	Recovery
	[mJ/m^2]							%
31.1	42.0	9.1	–42.0	10.9	0.9	6.4	–42.2	46.4
31.2	42.4	5.3	–51.9	6.1	0.9	4.7	–50.3	49.3
32.1	44.3	3.9	–55.3	4.8	0.9	1.2	–58.1	46.4
32.2	47.3	3.6	–54.3	3.1	0.0001	0.04	–63.6	52.0

The relatively small polar component of the free surface energy of coals causes that the value of water spreading work W_S is negative and changes from –42 to –54,3 mJ/m^2 for the types 31.1 and 32.2, respectively, therefore the natural floatability of these coals is relatively high. The flotation tests carried out in the Hallimond tube showed that their natural floatability (for the fractions with a grain size of 0.12–0.2 mm) confirmed it because the recoveries were 46%–52% [46]. According to the studies carried out by Jańczuk [66], the presence of apolar collector (*n*-octane) on the coal surface causes a significant decrease of water adhesion to the coal surface, thus facilitating the contact of air bubble with the coal surface, which is reflected in the flotation process.

The flotation results of the coals against their surface coverage with *n*-nonane obtained by us [46] are presented in Fig. 6.

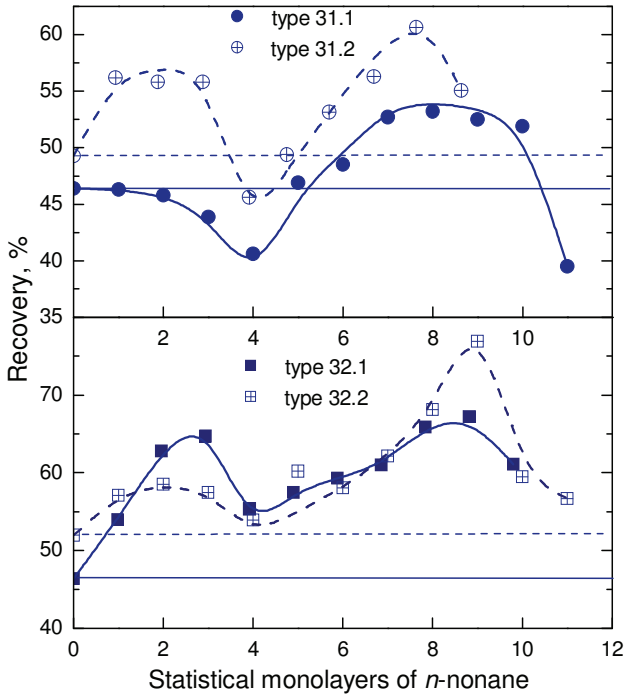

Fig. 6. Floatation recovery changes of different type of coals as a function of number of statistical monolayers of *n*-nonane (1.5 g samples floated with 100 cm^3 of nitrogen). Reproduced from Ref. [46].

There are minima and maxima of the recoveries which are characteristic of hydrophobic solids [39, 40]. The observed changes in floatability probably result from a heterogeneous coverage of coal surfaces with the collector and/or partial removal of the *n*-nonane

from the coal surface. This caused changes in the *n*-nonane film structure. Therefore, even several statistical monolayers of *n*-alkane do not cause complete hydrophobization which would appear in a 100% flotability. Although these coals are characterized by a lower hydrophobicity, still a similar behaviour was observed.

4. HYDROPHILIC SOLIDS: QUARTZ, MARBLE, BARITE

The results of flotability changes as a function of surface coverage with suitable collectors of quartz, marble, barite are presented in Figs. 7–14. Moreover, there are plotted changes of the polar γ_S^p and γ_S^d components calculated from the Owens and Wendt's approach (Eq. (4)) (Figs. 7–10) or γ_S^{LW}, γ_S^- and γ_S^+ calculated from the van Oss et al.'s approach (Eq. (5)) (Figs. 12 and 13) [4, 43, 44].

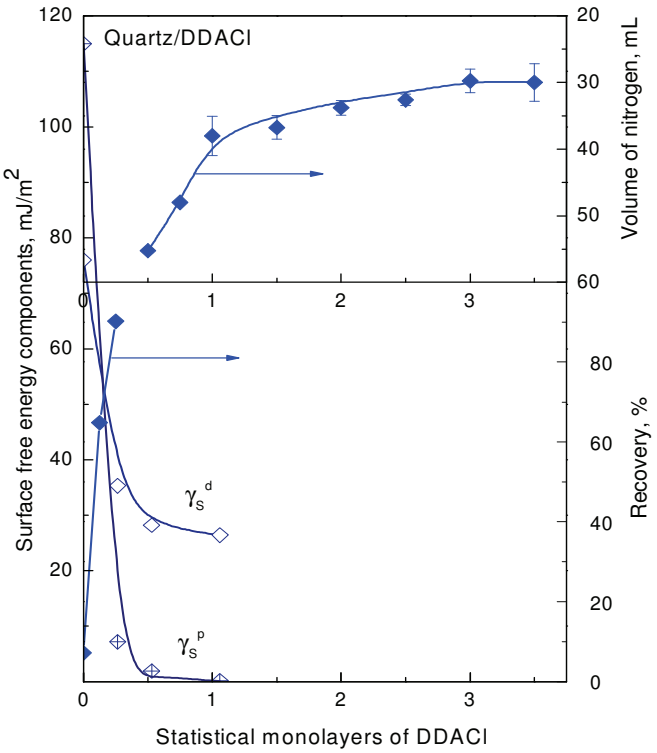

Fig. 7. Changes in the dispersion (γ_S^d) and polar (γ_S^p) components of surface free energy and flotability of quartz as a function of its surface precoverage with DDACl. (1.5 g samples floated with 100 cm^3 of nitrogen if noncomplete flotation). Note: already at 1 statistical monolayer coverage the polar component γ_s^p vanished zero and was the zero up to 3 statistical monolayers. It allowed completely flotation of the sample with 30 cm^3 of N_2.

Fig. 7 presents the results for quartz covered with dodecyl amine chloride (DDACl). The quartz sample (1.5 g) floated completely at the 0.5 monolayer coverage with 55 mL of nitrogen [2]. At this coverage the polar component was already reduced to 1.9 mJ/m^2 from 115 mJ/m^2 of the bare surface. The polar interactions are responsible for the quartz flotation activity. At a higher coverage of the surface with DDACl (up to 3 statistical monolayers) the polar components are reduced to zero and the sample is floated completely by 30 mL of nitrogen. Already at the one-monolayer coverage the work of spreading W_S was negative –90 mJ/m^2 (the thermodynamic condition fulfilled) while that for the bare surface it amounted to +89 mJ/m^2 (natural flotability 8% with 100 mL of nitrogen) (Fig. 11).

The analogous results for marble are plotted in Fig. 8 where tetradecylamine chloride (TDACl) was applied as the collector.

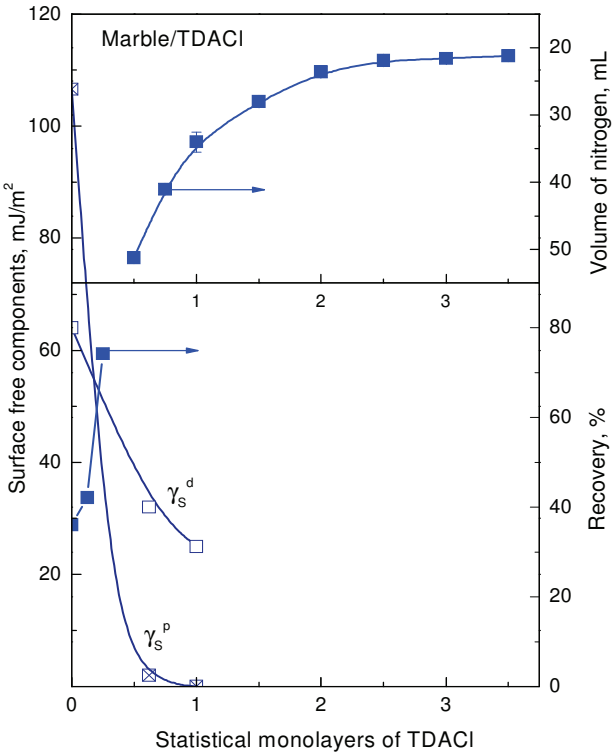

Fig. 8. Changes in the dispersion (γ_S^d) and polar (γ_S^p) components of surface free energy and flotability of marble as a function of its surface precoverage with TDACl. (1.5 g samples floated with 100 cm^3 of nitrogen if noncomplete flotation). See note at Fig. 7 and text below.

The 100% flotability of the 1.5 g sample with 51 mL of nitrogen at the surface coverage 0.6 monolayer of the collector was achieved. This corresponded to the drastic decrease of γ_S^p component from 107 mJ/m^2 to below 2 mJ/m^2. The maximum flotation activity was achieved at 2 monolayers coverage with TDACl where the whole sample was floated out with 23 mL of nitrogen. The work of spreading W_S changed from ca. 0 mJ/m^2 (36% natural flotability) to ca. –80 mJ/m^2 (at 0.6 TDACl monolayer) (Fig. 11).

In the case of barite both cationic and anionic collectors can be used [67], for example cationic TDACl [43, 44] or anionic sodium dodecyl-sulfate (SDS) [4, 44]. The results of flotation activity changes and the surface free energy components if anionic collector is shown in Fig. 9.

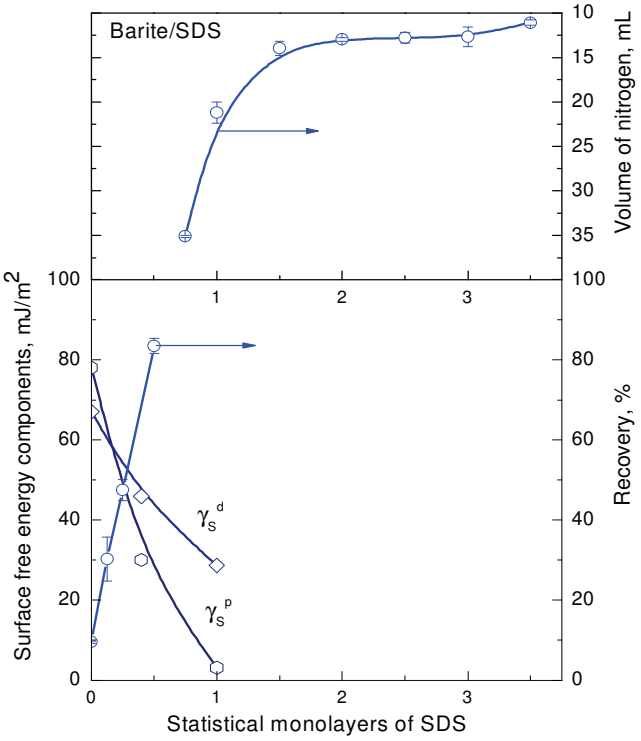

Fig. 9. Changes in the dispersion (γ_S^d) and polar (γ_S^p) components of surface free energy and flotability of barite as a function of its surface precoverage with SDS. (1.5 g samples floated with 100 mL of nitrogen if noncomplete flotation). See note at Fig.7 and the text below.

Natural flotability of the used barite sample was 10% and the complete flotation of 1.5 g sample was achieved using 35 cm^3 of

nitrogen at the 0.75 statistical monolayer coverage where the polar component γ_S^p amounted to ca. 15 mJ/m^2. However, at 1 monolayer its value decreased to 3 mJ/m^2 and only 21 cm^3 of nitrogen floated the whole sample. At the 2 monolayers coverage the maximum flotation activity was obtained which was reflected in 13 cm^3 of nitrogen needed to complete the sample flotation [4].

The results with the cationic collector TDACl are presented in Fig. 10.

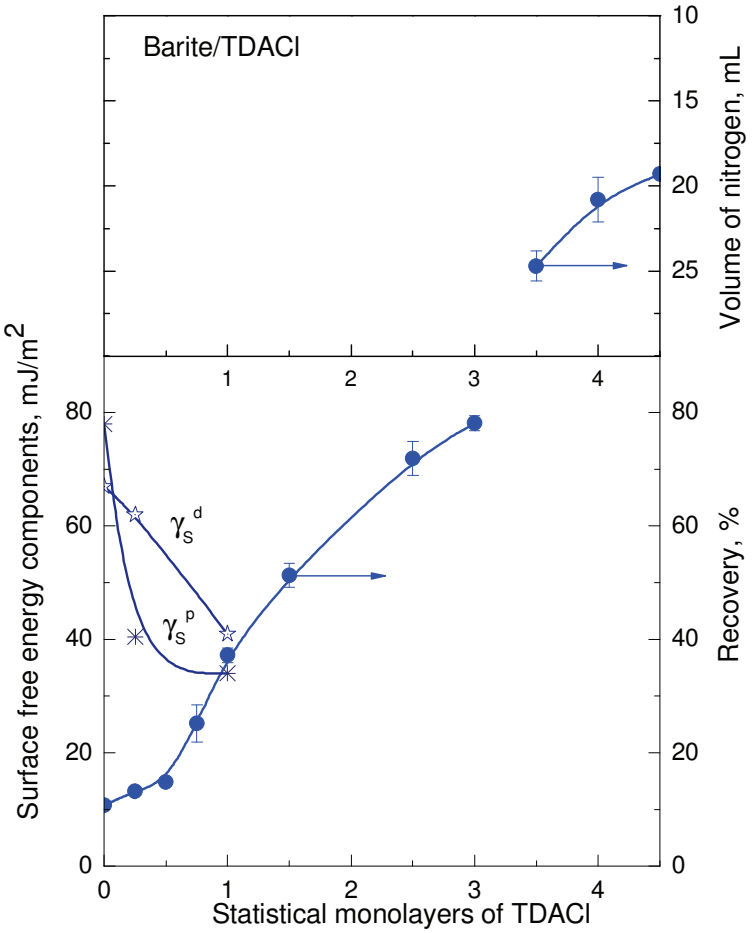

Fig. 10. Changes in the dispersion (γ_S^d) and polar (γ_S^p) components of surface free energy and flotability of barite as a function of its surface precoverage with TDACl. (1.5 g samples floated with 100 cm^3 of nitrogen if noncomplete flotation). Note: at 1 statistical monolayer coverage with this cationic surfactant the polar component is still relatively big. It means that the coverage is not uniform. See text below.

Comparing these results with those from Fig. 9 where the anionic SDS collector was used, it can be clearly seen that the cationic

collector is much less efficient that the anionic one. The complete flotation of the barite sample was obtained at as much as 3.5 statistical monolayers coverage with the cationic collector, where 25 mL of nitrogen was consumed. At 1 statistical coverage of the surface with this collector the barite flotation recovery was only 37% and the polar component was as high as 34 mJ/m^2. This means that actually the surface had not been covered uniformly with the collector [4, 43].

As already mentioned, determination of the work of solid-liquid adhesion (water) and knowledge of the work of liquid cohesion (water) allows to predict the thermodynamic capability of the flotation. A decisive role for the efficiency of the froth flotation is decrease of the interactions of solid/water, i.e. selective hydrophobization of surface particles by the collector which indicates a significant decrease of the work of water adhesion W_A, and in consequence, appearance of negative work of spreading W_S.

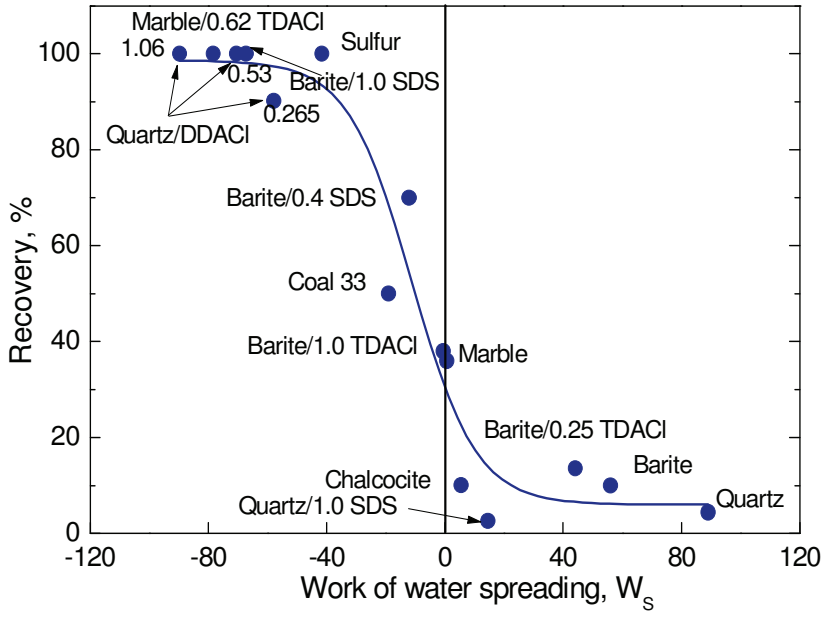

Fig. 11. Flotation recovery of some minerals and rocks (natural and with precovered of collectors) vs. of work of water spreading (O-W approach). Reproduced from Ref. [6].

Fig. 11 presents the floatability of various solid samples as a function of W_S, which was calculated using the dispersive γ_S^d and polar γ_S^p components of their surface free energy determined from the Owens and Wendt approach [6, 56]. In the figure the vertical line

shows W_S=0, which is the limit of good and poor flotability of the solids on the left and right sides, respectively. Obviously, there is a transition region between the good and poor flotability.

Using the van Oss et al.'s approach [57] and measuring the zeta potentials and contact angles of the barite samples, which were powdered for the zeta potential measurements or compressed for the contact angle measurements, the solid surface free energy components were determined [4]. The relationships between the flotability and the surface free energy components changes are presented in Fig. 12 for the barite precovered with up to 1 statistical monolayer of SDS.

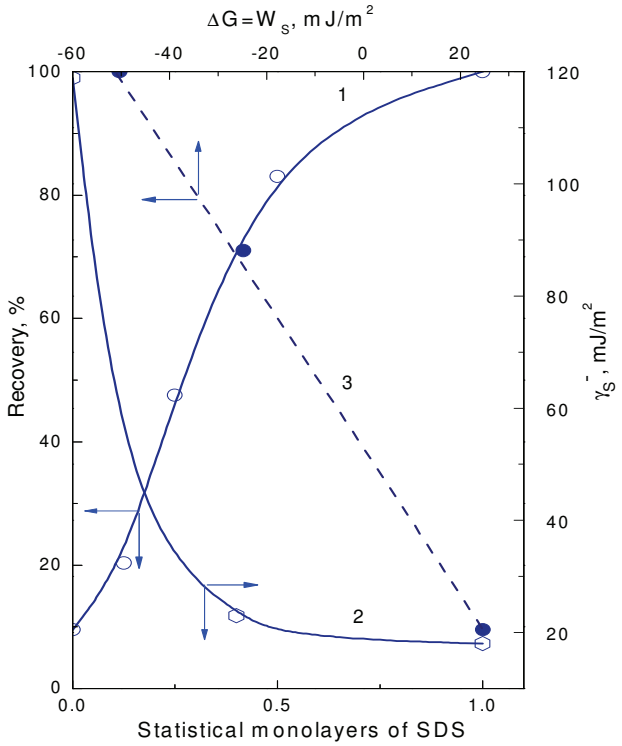

Fig. 12. Changes in flotability (curve 1), and electron-donor parameter (γ_S^-) (curve 2) as a function of surface precoverage with SDS and the relationship between recovery and $\Delta G = W_S$ changes of the barite samples (curve 3). Reproduced from Ref. [4].

The interdependence of the changes in the electron donor parameter γ_S^-, flotation recovery and the Gibbs' free energy (work of water spreading) $\Delta G = W_A - W_C = W_S$ can be evidently seen. The linear relationship of the energy and flotability was found and a sharp

decrease of the electron-donor parameter is reflected in a sharp increase in the flotation recovery, from 10% (bare surface) to 100% at one monolayer SDS coverage. These relationships characterize fully the thermodynamics of the flotation process.

Fig. 13 shows the changes in floatability and the apolar γ_S^{LW} and polar γ_S^- components of surface free energy for barite via its surface precoverage with TDACl up to 1 monolayer [44].

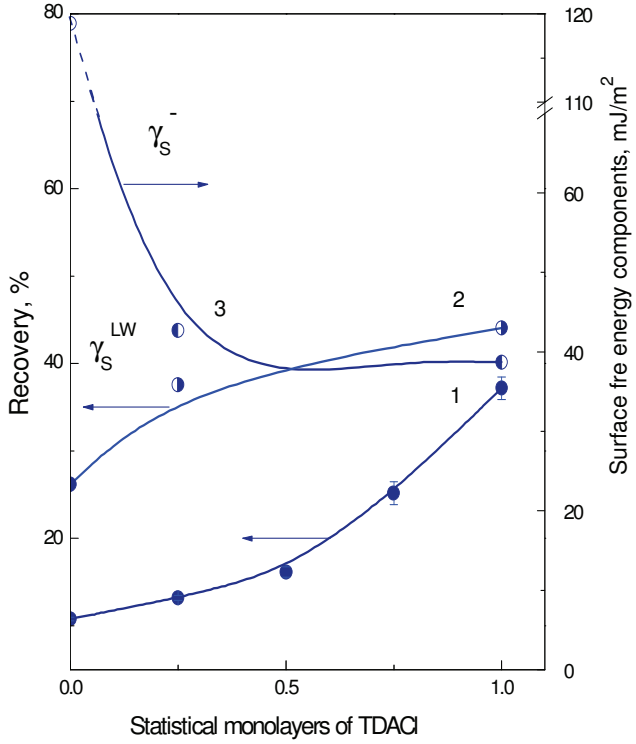

Fig. 13. Changes of flotability (curve 1), apolar γ_S^{LW} (curve 2) and polar γ_S^- components of surface free energy (curve 3) of barite as a function of its surface precoverage with TDACl. Reproduced from Ref. [44].

The adsorbing molecules of cationic collector on the barite surface influence its hydrophilic properties (the increase of apolar and decrease in polar interactions, especially of the electron-donor parameter). It can be assumed that the ionic species of TDACl or its neutral molecules adsorbing on the selected surface sites do not form a uniform monolayer but rather a mosaic structure (hemimicelles (aggregates) [19]. At the one statistical monolayer of the collector it should result in increased dispersion interactions. However, the resulting hydrophobicity of the surface rather does not achieve the energy value characteristic of a hydrocarbon chain, i.e. about 25

mJ/m^2. The polar electron-donor parameter γ_S^- is due to the presence of oxygen atoms on the mineral surface and it is responsible for the hydrophilic character of the barite surface. The decrease in γ_S^- from 119 mJ/m^2 (bare surface) to 36.8 mJ/m^2 at 1 monolayer coverage with TDACl causes an increase in the floatability from 10% to 38% at ΔG = –16 mJ/m^2.

In order to verify the determined components of surface free energy of barite [4], further investigations of the surface free energy of this mineral were carried out using the thin layer column (TLC) method and measurements of contact angles of water, formamide and glycerol [6]. For the experiments fine barite powder (smaller grains than described before) were used in both TLC and contact angle measurements on the compressed pellets. There were obtained the following components of surface free energy of bare surface of the barite: from contact angles γ_S^{LW} = 47.5±0 mJ/m^2, γ_S^-=54.8±2,4 mJ/m^2 and γ_S^+ = 0.25±0,2 mJ/m^2 and from the TLW method γ_S^{LW} = 48,6±1.3 mJ/m^2, γ_S^-=57.8±0.1 mJ/m^2 and γ_S^+ = 0.07±0.04 mJ/m^2. As can be seen the surface free energy components determined by the two different methods are very similar.

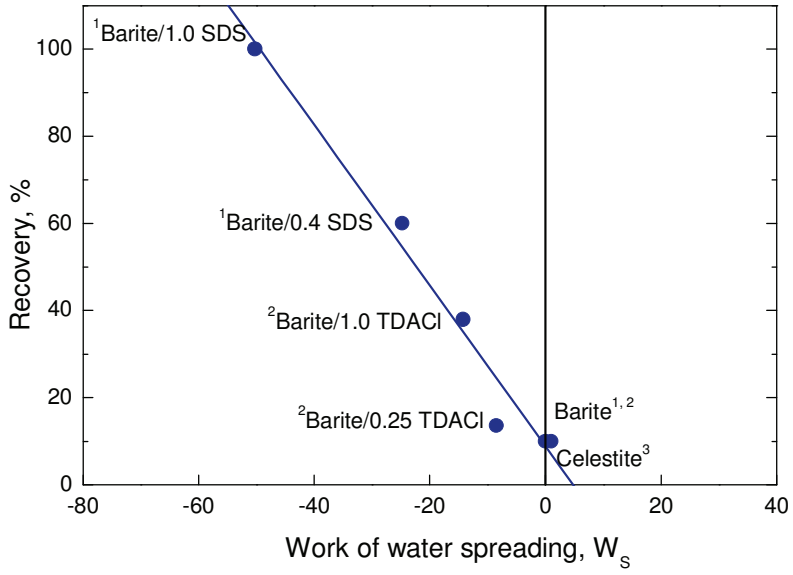

Fig. 14. Flotation recovery of barite samples (natural and with precovered of collectors) vs. of work of water spreading (van Oss et al. approach). Reproduced from Ref. [6].

From the determined components of the barite sample [6], and this barite sample covered with TDACl or SDS [4, 43] the work of

water spreading W_S values were calculated. The relationship between the flotation activity of bare barite and the samples covered by both collectors and the work of spreading W_S is presented in Fig. 14. For comparison the flotation of bare celestite, for which the components of the surface free energy were determined by the TLW method [45], is also shown. As can be seen, when the work of water spreading to the barite or celestite surface is close to zero (the work of water adhesion is close to the work of water cohesion) the flotability of these minerals is low and amounts to about 10%.

The increase in the negative value of W_S is accompanied be the increase in the recovery up to 100% for the barite sample precovered with 1 statistical monolayer of SDS, with a significant decrease of γ_S^- parameter from 57.4 to 18.0 mJ/m^2. Roughly a linear dependence of the free energy W_S and the changes in floatability are observed in the range of the surface coverage from 0 to 1 statistical monolayer of TDACl or SDS. During the flotation process of the barite sample, especially at its large coverage, partial desorption of the collectors into the solution took place, therefore the amount of collector remaining on the surface was actually smaller.

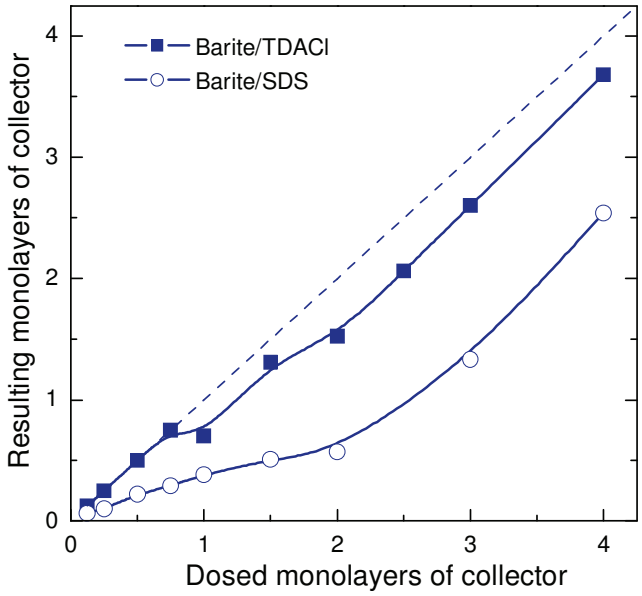

Fig. 15. Relationship between the initially deposited number of collector monolayers surface and that resulting after the flotation tests. Reproduced from Ref. [4].

This is shown in Fig. 15 [4]. In the case of SDS from the surface covered with 1 statistical monolayer 0.6 monolayer desorbed, while for TDACl the desorption was smaller and amounted only to about 0.3 monolayer. Nevertheless SDS appeared to be a more efficient collector because it blocks the polar adsorption centres on the surface (hydrogen bonding between the barite surface and water molecules) more efficiently than TDACl which results in a stronger contact of the gas bubble with the mineral particle.

4. SUMMARY

The presented results show clearly that besides of very important practical applications of flotation process of mineral ores and rocks beneficiation also it is very useful for fundamental study of hydrophobic/hydrophilic properties of solid surface. This is due to a very simple setup needed to conduct the experiments, i.e. single bubble Hallimond's tube. Moreover, such study allows also explanation thermodynamically the required energetic conditions for the flotation process to be efficient. The above results deal with both naturally hydrophobic and hydrophilic solid (minerals and rocks) surfaces. The application of a suitable collector causes surface hydrophobization which was shown in connection with the solid surface free energy changes and the resulting work of water adhesion to the surface. In consequence, it was conversion from positive to negative work of spreading over a given solid surface. Quantitative results presented in this paper for many solids explain completely the thermodynamic relations accompanying the flotation process.

REFERENCES

[1] A.F. Hallimond, *Mining Magazine,* **70**, 87, (1944).
[2] E. Chibowski, L. Hołysz, *J. Colloid Inter. Sci.,* **68**, 15, (1986).
[3] J. Drzymała, T. Chmielewski, K. L. Wolters, D. H. Birlingmair, T.D. Wheelock, *Trans. IMM, Sec. C*, **101**, C17, (1992).
[4] L. Hołysz, E. Chibowski, *Langmuir*, **8(1)**, 303, (1992).
[5] J. Drzymała, *Miner. Eng.,* **12**, 329, (1999).
[6] E. Chibowski, L. Hołysz, *Annales Universitatis Mariae Curie-Sklodowska Lublin - Polonia*, LIV/LV8, SECTIO AA, 117, (2000).

[7] T. Sreenivas, N.P.H. Padmanabhan, *Colloids Surf. A*, **205**, 47, (2002).
[8] P. Somasundaran, L. Zhang, *J. Petro. Sci. Eng.*, **52**, 198, (2006).
[9] A. Ansari, M. Pawlik, *Miner. Eng.,* **20**, 609, (2007).
[10] G. Bulut, S. Atak, E. Tuncer, *Canadian Metallurgical Quarterly* **47**, 119, (2008).
[11] D. Szyszka, E. Flapiak, J. Drzymała, *Physicochem. Probl. Miner. Process.*, **42**, 85, (2008).
[12] D.W. Fuerstenau, *Mining, Metallurgy & Exploration* **30,** 1, (2013).
[13] P. B. Kowalczuk, *Int. J. Miner. Process.*, **140**, 66, (2015).
[14] J. Drzymała, A. Swebodzińska, M. Duchnowska, A. Bakalarz, A. Łuszczkiewicz, P. B. Kowalczuk, *MEC 2016*, *E3S Web of Conferences*, **8**, 01031, (2016).
[15] J. W. Drelich, *Physicochem. Probl. Miner. Process.*, **54(1)**, 10, (2018).
[16] M.C. Fuerstenau, G.J. Jameson, R.H. Yoon, Froth Flotation: a Century of Innovation, SME, Littleton, 2007.
[17] J. Drzymała, *Adv. Colloid Interface Sci.,* **50**, 143, (1994).
[18] J.S. Laskowski, *Canadial Metallurgical Quarterly,* **46(3)**, 251, (2007).
[19] J.W. Drelich, Contact angles measured at mineral surfaces covered with adsorbed collector layer. *Miner. Metal. Proc.*, **18(1)**, 31, (2001).
[20] A. Bastrzyk, I. Polowczyk, E. Szeląg, Z. Sadowski, *Physicochem. Probl. Miner. Process.*, **42**, 261, (2008).
[21] A. Szymańska, Z. Sadowski, *Adsorption*, **16**, 233, (2010).
[22] A.M. Didyk, Z. Sadowski, *Physicochem. Probl. Miner. Process.*, **48(2)**, 607, (2012).
[23] E. Potapova, X. Yang, M. Grahn, A. *Colloids Surf. A*, **386**, 79, (2011).
[24] G. Liu, X. Yang, H. Zhong, *Adv. Colloid Interface Sci.*, **246**, 181, (2017).
[25] Y. Xing, X. Gui, F. Karakas, Y. Cao, *Minerals*, **7(11)**, 223, (2017).
[26] M.M. Fawzy, *Physicochem. Probl. Miner. Process.*, **54(1)**, 10, (2018).
[27] Z. Liu, Y. Liao, M. An, Q. Lai, L. Ma, Y. Qiu, *Physicochem. Probl. Miner. Process.,* **54(3)**, 677, (2018).
[28] A. Pattanik, R. Venugopal, *Colloid Interface Sci. Communications*, **25**, 41, (2018).
[29] J.S. Laskowski, *Miner. Process. Extractive Metall. Rev.*, **5(1-4)**, 25, (1989).
[30] M. Rudolph, R. Hartman, *Colloids Surf. A,* **513**, 380, (2017).
[31] J. Drzymała, *Inter. J. Miner. Process.*, **42(3-4)**, 139, (1994).
[32] J. Drzymała, *Inter. J. Miner. Process.*, **42**, 153, (1994). Erratum, *Inter. J. Miner. Process.* **43**, 135, (1995).
[33] J. Drzymała, *Inter. J. Miner. Process.*, **55**(3), 203, (1999).
[34] L.K. Koopal, T. Goloub, A. de Keizer, M. P. Sidorova, *Colloids Surf. A*, **151**, 15, (1999).
[35] J. Drzymała, J. Lekki, *J. Colloid Interface Sci.*, **130**, 205, (1989).

[36] M. Watanabe, P. B. Kowalczuk, J. Drzymała, *Physicochem. Probl. Miner. Process.*, **46**, 13, (2011).
[37] P.B. Kowalczuk, O. Sahbaz, J. Drzymała, *Miner. Eng.*, **24,** 766, (2011).
[38] P.B. Kowalczuk, J. Drzymała, *I&EC Research,* **50**, 4207, (2011).
[39] E. Chibowski, L. Hołysz, P. Staszczuk, *Polish J. Chem.*, **59**, 1167, (1985).
[40] E. Chibowski, L. Hołysz, *J. Colloid Inter. Sci.*, **127(2)**, 377, (1989).
[41] E. Chibowski, L. Hołysz, *Fuel*, **8(1)**, 1280, (1989).
[42] E. Chibowski, L. Hołysz, *J. Adhes. Sci. Technol.*, **3(8)**, 575, (1989).
[43] E. Chibowski, L. Hołysz, *J. Mat. Sci.*, **27**, 5221, (1992).
[44] E. Chibowski, L. Hołysz, *Prog. Colloid & Polym. Sci.*, **89**, 173, (1992).
[45] L. Hołysz, *Polish J. Chem.,* **68**, 2699, (1994).
[46] L. Hołysz, *Fuel*, **75(6)**, 737, (1996).
[47] F. González-Caballero, E. Chibowski, L. Hołysz, J.M. Bruque, *Colloids Surf.*, **35(1)**, 65, (1989).
[48] S. Calgaroto, A. Azevedo, J. Rubio, *Inter. J. Miner. Process.,* **137**, 64, (2015).
[49] S.R. Rao, J. Leja, Surface Chemistry of Froth Flotation, 2 nd Ed.; Kluwer Academic/Plenum Publisher: New York, Vol. 2, 2004.
[50] M. Humeres, N.S. Dabacher, T. Wagner, G. Gonzalez, *Sep. Sci. Technol.*, **27(7)**, 1501, (1993).
[51] X. You, L. Lin Li, X. Lyu, *Physicochem. Probl. Miner. Process.*, **53(1)**, 333, (2017).
[52] J. Laskowski, in: Separation Technologies for Minerals, Coal, and Earth resources. C.A. Young and G.H. Lutterell Eds. SME. USA, p. 7, 2012.
[53] A.W. Adamson, A.P. Gast, Physical Chemistry of Surfaces, 5th ed.; New York: Wiley & Sons, 1997.
[54] A. Duprè, *Gauthier-Villars*, Paris, p. 368, (1869).
[55] T. Young, *Philosophical Transactions of the Royal Society of London*, **95**, 65, (1804).
[56] D.K. Owens, R. Wendt, *J. Appl. Polym. Sci.,* **13**, 1741, (1969).
[57] C.J. van Oss, M.K. Chaudhury, R.J. Good, *Chem. Rev.*, **88(6)**, 927, (1988).
[58] B. Jańczuk, W. Wójcik, T. Białopiotrowicz, *Croatica Chemica Acta*, **61(1)**, 51, (1988).
[59] B. Jańczuk, W. Wójcik, A. Zdziennicka, *Powder Technol.*, **76(3)**, 233, (1993).
[60] W. Wójcik, T. Białopiotrowicz, B. Jańczuk, *Fuel*, **67(5)**, 688, (1988).
[61] B. Jańczuk, E. Chibowski, T. Białopiotrowicz, L. Hołysz, A. Kliszcz, *Clay Clay Miner.*, **38(1)**, 53, (1990).
[62] C. Karagüzel, M.F. Can, E. Sönmez, M.S. Celik, *J. Colloid Interf. Sci.*, **285(1)**, 192, (2005).
[63] W. Wójcik, T. Białopiotrowicz, B. Jańczuk, *Fuel*, **69(5)**, 207, (1990).

[64] T.A. Solov'eva, A.N. Muklakova, *Fuel Energy Abstracts,* **36(4)**, 246, (1995).
[65] B. Jańczuk, *Przem. Chem.*, **72(3)**, 103, (1993).
[66] B. Jańczuk, *Fuel*, **65(1)**, 113, (1986).
[67] M. Kecir, A. Kecir, *J. Polish Miner. Eng. Soc.*, **17(2)** 269, (2016).